On the Transformation of a Tropical Easterly Wave into a Tropical Depression: A Simple Numerical Study

YOSHIO KURIHARA

Geophysical Fluid Dynamics Laboratory/NOAA, Princeton University, Princeton, NJ 08542

MITSUHIRO KAWASE

Geophysical Fluid Dynamics Program, Princeton University, Princeton, NJ 08542

(Manuscript received 11 October 1983, in final form 2 October 1984)

ABSTRACT

Through the time integration of a simple numerical model, the transformation of a tropical easterly wave into a tropical depression was investigated. The initial condition selected for the model is a slowly decaying, adiabatic linear normal mode resembling an easterly wave. It was found that the addition of a CISK (conditional instability of the second kind) type heating effect to the model results in the growth of the wave. Addition of the nonlinearity effect alone, which includes the nonlinear zonal advection and vertical stretching of relative vorticity, has little impact on the wave evolution. However, if the above nonlinearity effect is combined with the heating effect, it can cause the contraction of the disturbance and enhance the development. The initial free wave undergoes significant structural changes during its transformation into a developing system.

Experiments were also performed for three different waves under various basic flow conditions. The obtained results agree with a conclusion of the three-dimensional simulation experiments by Tuleya and Kurihara; the coupling between the upper-level wind and the propagating disturbance at low levels may be an important mechanism in the formation of a tropical depression in the trough region of an easterly wave.

1. Introduction

The purpose of this study is to investigate a mechanism of transformation of tropical easterly waves, which are viewed here as possible causes of tropical depressions. Over the warm ocean in the tropics, a depression develops in many cases at or in the vicinity of the trough of an easterly wave (e.g., Yanai, 1961). Various factors contribute to such a transformation of easterly waves. One of them is the nonlinearity effect working on a vertical plane, which includes the nonlinear vorticity stretching suggested by Hoskins (1975) as a mechanism for the formation of a midlatitude front in a baroclinic wave. On the other hand, the numerical simulation study by Kurihara and Tuleya (1981) suggests that a tropical depression may not form within an easterly wave without the effect of diabatic heating. In the present numerical study, we evaluate the individual as well as combined roles of the above two effects in the transformation of tropical easterly waves. It should be noted here that the formation of tropical depressions may also be triggered by other mechanisms, which are omitted or not entirely considered in this study, such as the barotropic instability of the basic flow and the nonlinear advection of relative vorticity on a horizontal plane as hypothesized by Shapiro (1977).

In Section 2, a simple dynamical model of easterly waves, the initial conditions of the model and the design of numerical experiments are described. The results of time integrations are presented and discussed in Section 3. In Section 4, the results of the supplemental experiments performed under various conditions are summarized. Some remarks related to this study are made in Section 5.

2. A numerical model of easterly waves

a. Governing equations

We assume that the wave we treat is governed by the primitive equations on a β-plane and is uniform in the meridional direction, i.e., $\partial/\partial y = 0$ for all variables at all times. A wave disturbance is superposed on the zonal flow which is dependent on pressure: $U(p)$. Both $U(p)$ and the potential temperature $\Theta(p)$ of a basic state can be arbitrarily specified. The meridional variation of the basic flow is not considered for the sake of simplicity. The experiments by Tuleya and Kurihara (1981) suggest that a tropical depression can be formed without the horizontal shear of the basic flow, while the cyclonic shear of the low-level basic flow and, to a less degree, the anticyclonic shear of the upper-level flow can enhance the development of disturbances. It seems, however, that the meridional

change of basic flow, together with the horizontal tilt of the wave axis, can play an important role in the energetics of certain tropical waves (e.g., Reed, 1979). Also, the evolution of depressions in the area of monsoon troughs may strongly be influenced by the horizontal shear of the basic flow. The present model cannot handle these systems.

In the x (zonal)–y (meridional)–p (pressure) coordinate system, the components of the perturbation wind are expressed by u (the eastward wind), v (the northward wind) and ω (vertical p–velocity). Then, the equations for the perturbation vorticity ζ $(=v_x)$ and the divergence D $(=u_x)$, the continuity equation, the tendency equation for the perturbation geopotential of the 1000 mb surface ϕ^* (asterisk is used to indicate a value at the 1000 mb level), the hydrostatic equation and the equation for perturbation potential temperature θ are written as follows:

$$\zeta_t = -U\zeta_x - fD - \beta v + K\zeta_{xx} - c\zeta - a[(u\zeta)_x + (\omega v_p)_x]; \quad (1)$$

$$D_t = -UD_x - \phi_{xx} + f\zeta - \beta u - U_p\omega_x + KD_{xx} - cD - a[(uD)_x + (\omega u_p)_x]; \quad (2)$$

$$D + \omega_p = 0; \quad (3)$$

$$\phi_t^* = -U\phi_x^* + fUv + \alpha^*\omega - au\phi_x^*; \quad (4)$$

$$\partial\phi/\partial \ln p = -R\pi\theta; \quad (5)$$

$$\theta_t = -U\theta_x + Bv + S\omega + K\theta_{xx} - a[(u\theta)_x + (\omega\theta)_p] + bQ, \quad (6)$$

where the subscripts indicate derivatives, ϕ is the perturbation geopotential of an isobaric surface, R the gas constant, $\pi = (p/p_0)^{R/c_p}$ [p_0 is the standard pressure (1000 mb) and c_p the specific heat of air at constant pressure], f the Coriolis parameter, $\beta = \partial f/\partial y$ and α^* the specific volume at the 1000 mb level. Additionally, S is the static stability parameter [$S(p) = -\Theta_p$]; B the measure of baroclinicity [$B(p) = -\Theta_y = -(f/\pi R)(\partial U/\partial \ln p)$], K the horizontal diffusion coefficient and c the coefficient for damping due to the surface friction. The beta terms are included in (1) and (2) so that the Rossby waves propagate in a proper manner in the present system. As suggested by Tuleya and Kurihara (1981), the evolution of a wave may well be influenced by its own phase speed.

In the prognostic Eqs. (1), (2), (4) and (6), the trace parameter a is attached to the nonlinear terms; the parameter b is attached to the quantity Q, which represents the effect of diabatic heating. With $a = b = 0$, the equations are reduced to an adiabatic, linear system. The nonlinearity and the heating effects can be added to the system by setting a and b to unity.

In this study, we investigate how a wave in the linear system is transformed with the addition of nonlinearity and heating effects. In particular, we imagine a situation in which a neutral or slowly decaying easterly wave in the tropics is converted into a system capable of producing a tropical depression.

b. *Normal modes of a linear system*

Normal modes of the linear system (1)–(6) with $a = b = 0$ having a prescribed wavelength can be obtained by solving an eigenvalue problem once all the coefficients of the equations are given. As was done by Kurihara (1976) in the eigenvalue analysis of the hurricane spiral bands, the perturbation variables are defined at discrete pressure levels and finite differencing is applied to treat the derivatives with respect to p. The pressure levels chosen are 100, 300, 500, 700, 900 mb levels for ζ, D, ϕ, u and v; 200, 400, 600, 800 mb levels for θ and ω (θ and ω at 0 mb are fixed at zero, respectively); 1000 mb level for all above variables and ϕ^*, making the number of prognostic quantities 18. Accordingly, 18 free modes exist, in general, for a given wave scale.

The basic fields used in the present study are shown in Table 1. According to the results of a numerical study by Tuleya and Kurihara (1981), these fields are favorable for tropical cyclogenesis. Note that the basic flow is easterly at all levels; it is -5 m s^{-1} at the surface and its speed increases moderately with height. Furthermore, the following constants are used

TABLE 1. Specification of basic fields.

P (mb or hPa)	U (m s^{-1})	U_p (10^{-5} m s^{-1} Pa^{-1})	T (K)	S (10^4 K Pa^{-1})	B (10^{-7} K m^{-1})
100	−12				
200		5	218.3	6.6332	−2.499
300	−11				
400		10	255.9	6.8548	−8.817
500	−9				
600		10	275.1	6.3272	−11.922
700	−7				
800		10	288.2	4.6822	−14.702
900	−5				
1000	−5	0	299.6	3.7863	0

to determine the coefficients of the equations: $R = 287$ J kg^{-1} K^{-1}, $R/c_p = 2/7$, $f = 4.97 \times 10^{-5}$ s^{-1}, $\beta = 2.14 \times 10^{-11}$ m^{-1} s^{-1}, $\alpha^* = 0.86$ m^3 kg^{-1}, $K = 1 \times 10^3$ m^2 s^{-1} and $c = 1 \times 10^{-5}$ s^{-1} (at 1000 mb level only; zero elsewhere).

Adiabatic, linear normal modes in the previously described basic fields were obtained for the wavelength of 2500 km, a typical zonal scale of an easterly wave. Of 18 total solutions obtained, 12 solutions correspond to the inertial–gravity wave modes modified by the basic flow and the other 6 to Rossby-like modes showing fairly small intrinsic phase speeds. Every mode decays with a negative e-folding time between -36 and $-43\,883$ h. After comparing the structure of each mode with the observed feature of a tropical easterly wave (e.g., Wallace, 1971; Reed, 1979), a normal mode which most closely resembled an actual easterly wave was selected. This mode is one of the Rossby modes and is more or less confined below the 500 mb level. Its perturbation flow (u, v and ζ) is strongest at the 900 mb level and decreases with height, and its wave axis tilts eastward with height. It propagates to the west with the phase speed of 8.9 m s^{-1} and decays slowly with an e-folding time of -288.4 h. We use this wave, setting the amplitude of v at the 1000 mb level at 5 m s^{-1}, as an initial disturbance in the experiments.

c. *Design of experiments*

The shape and intensity of the initial wave can be progressively modified by the nonlinearity and/or heating effect. We investigate this process through the time integrations of the finite difference version of (1) through (6). The effect of nonlinearity can be included by setting the trace parameter a to one. Similarly, one can incorporate the heating effect by switching the parameter b from zero to one. Hereafter, the values of a and b used in each experiment will be shown by a symbolic expression EXP(a, b).

We design four numerical integrations as listed in Table 2. The disturbance dealt with in EXP(0, 0) is the slowly decaying easterly wave mentioned in the preceding subsection. Numerical results of this experiment can be compared with the known analytical solution so that the accuracy of the computational scheme may be checked. The effect of nonlinearity and that of diabatic heating are examined separately by EXP(1, 0) and EXP(0, 1) respectively. The two effects are combined in EXP(1, 1).

TABLE 2. List of numerical experiments.

EXP(a,b)	Main feature
EXP(0,0)	adiabatic, linear free wave
EXP(1,0)	effect of nonlinearity only
EXP(0,1)	effect of diabatic heating only
EXP(1,1)	combined effect of nonlinearity and heating

The form of the nonlinear terms in (1) and (2) indicates that although the nonlinearity can influence the local tendencies of ζ and D, the zonal average of the nonlinear effect over the entire extent of the wave vanishes. Accordingly, the zonal means of ζ and D remain zero in all experiments as long as the zonal averages of v and u are kept zero. Because of (3), the zonal average of ω becomes zero. The zonal average of the nonlinear term in (4) is not guaranteed to vanish. In order to preserve the total mass of the system, we adjust the computed local tendency of ϕ^* by subtracting its zonal average, which is usually quite small, at each step of time integration. The nonlinearity in (6) may cause changes in the zonal averages of θ and ϕ. We allow such changes to take place.

The heating term in (6) is formulated in a CISK (conditional instability of the second kind) type form:

$$Q(p) = -S(p)h(p)\omega_B, \tag{7}$$

where $\omega_B = 100$ mb $\times$ [D (1000 mb) + D (900 mb)]/2, and $h(p)$ at 200, 400, 600, 800 and 1000 mb are 0.0, 1.4, 1.9, 1.6 and 0.0, respectively. In a model with the heating term (7), behavior of a wave disturbance is influenced by a specified vertical profile of heating since the generation of the eddy available potential energy is dependent on the heat distribution within the wave. The specification of $h(p)$ in the present model is made on the basis of the results of numerical simulation of moist convection by Lipps (1983), personal communication). From the total heating rate in the air column, i.e., $c_p \int \pi Q dp/g$ (g: the acceleration of gravity), the boundary-layer mixing ratio of the present model is estimated to be 19.9×10^{-3}. It should be noted that the heating term is dependent on D; a CISK-type process can work as long as $-D$ and ζ are in phase. Since the nonlinear distortion of the divergence pattern does not occur in EXP(0, 1), the horizontal distribution of Q remains sinusoidal in this case. On the other hand, in EXP(1, 1), the interaction between the nonlinearity and the heating effects can lead to a large deformation of both the D and Q fields.

The numerical model is constructed so that the free wave at the initial time can be time integrated quite accurately in EXP(0, 0). The vertical division of the model and the arrangement of the variables at the discrete pressure levels are the same as those used in the calculation of normal modes (Section 2b). The zonal extent of the model domain is 2500 km, (the wavelength of the initial disturbance), and the cyclic boundary condition is assumed. A grid system with 62.5 km zonal resolution is used; the grids for u and v are placed between those for D and ζ. The spatial differencing is a scheme which does not give rise to a fictitious source of energy. To avoid a noisy distribution of Q, we derive ω_B in (7) from the three-point

horizontal average of D with the weights ¼, ½, ¼. The time integration of the model is carried out to 72 h with a 30 s time step by means of a two-step iterative scheme (Kurihara and Tripoli, 1976) in which the weights w_1 and w_2 are fixed at 0.506 and 2.5, respectively. Because of the above scheme, high frequency noises, if excited during the integration, can be damped quickly.

Performance of the linear portion of the numerical model was checked by the examination of the results obtained from EXP(0, 0). In this experiment, the maximum relative vorticity at 1000 mb decreases 22% in 72 h integration, from 1.25×10^{-5} s^{-1} to 0.98×10^{-5} s^{-1}. The above decay rate is in perfect agreement with the exact damping rate of the linear normal mode chosen for the initial condition of the model. This indicates an excellent level of accuracy of at least the linear portion of the computational scheme.

3. Transformation of a wave: Numerical results

a. Time variation of the surface vorticity

The initial wave resembling a tropical easterly wave evolves into different types of disturbances by responding to the different physical factors. Figure 1 shows the time variations of the maximum relative vorticity at 1000 mb in the three experiments. After 72 h, the initial value 1.25×10^{-5} s^{-1} increases to 5.14×10^{-5} s^{-1} in EXP(1, 1) and to 3.36×10^{-5} s^{-1} in EXP(0, 1), but decreases to 1.00×10^{-5} s^{-1} in EXP(1, 0). It is clear that the wave can develop with the aid of diabatic heating and that the development can be enhanced by the additional effect of the nonlinearity. The effect of nonlinearity alone does not cause the wave to intensify.

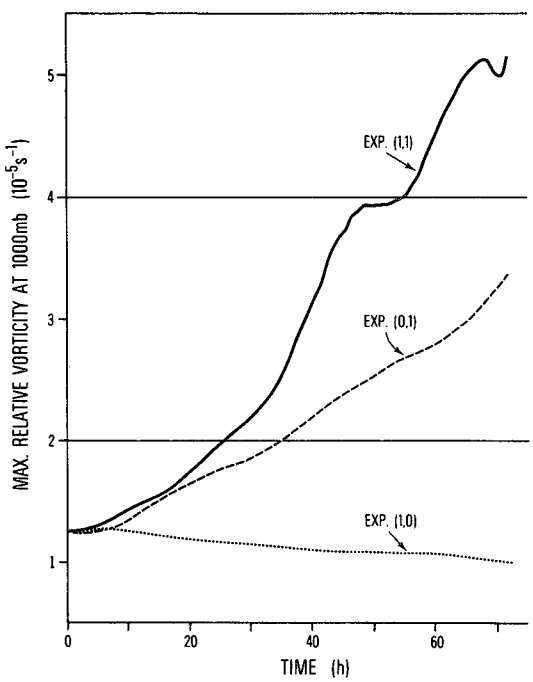

FIG. 1. Time variations of the maximum relative vorticity at 1000 mb for EXP(1, 0), EXP(0, 1) and EXP(1, 1).

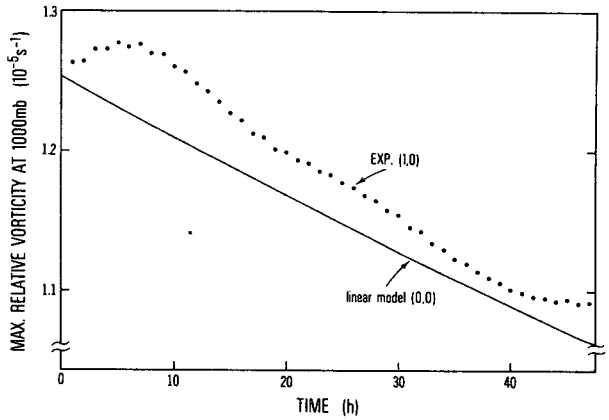

FIG. 2. As in Fig. 1, but for EXP(0, 0) and EXP(1, 0).

The initial increase of the surface vorticity in the trough region of the wave in EXP(0, 1) can be attributed to the warming of an air column and the subsequent increase in the surface convergence. The vorticity increase at the surface trough ensues as long as the effect of planetary vorticity stretching, $-fD$ in (1), exceeds the effect of frictional damping. As seen in Fig. 1, the surface vorticity in EXP(0, 1) increases at a nearly constant rate. The linearity of the equation system in EXP(0, 1) indicates that not only the surface vorticity but also the surface divergence and the depth of surface trough increase almost linearly with time. The simultaneous change of ϕ^*, or more specifically the increase of ϕ^*_{xx}, with the surface vorticity increase tends to maintain the flow in a nearly geostrophic equilibrium.

In Fig. 2, the decay of the disturbance in EXP(1, 0) is compared with the damping of the initial free wave. It is shown that the nonlinearity process increases the maximum vorticity until 7 h. The new vorticity field, however, is not in a nearly geostrophically balanced state since the simultaneous change in the ϕ-field is negligibly small. As a result, a positive tendency of D is induced, which is detrimental to a further increase of vorticity. The nonlinearity effect in EXP(1, 0) thus makes little impact on the disturbance structure and the disturbance tends to behave in a manner similar to the damping linear free wave, i.e., EXP(0, 0).

In EXP(1,1) we find that the change in the ζ-field proceeds concurrently with that in the ϕ-field. In such a case, the nonlinearity effect can significantly enhance the development of a wave. The above finding is consistent with the numerical results obtained from a three-dimensional simulation model of

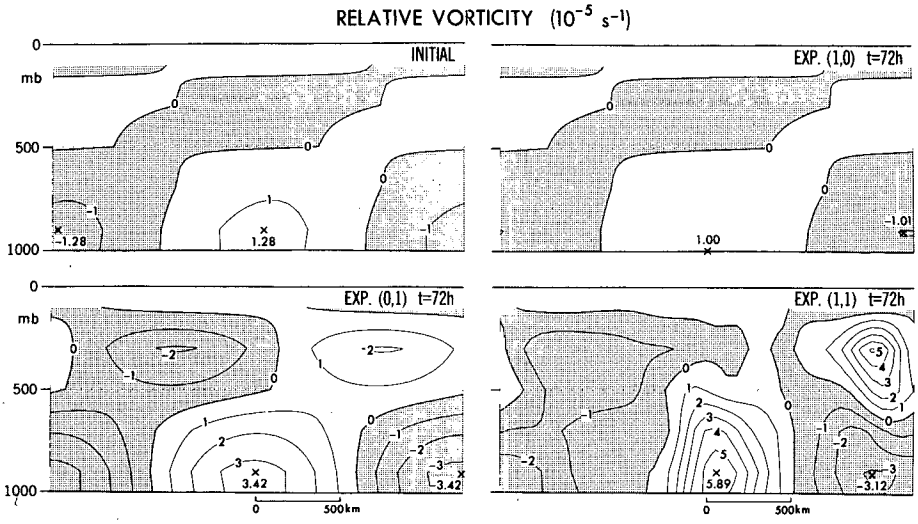

FIG. 3. Zonal-vertical distributions of relative vorticity (10^{-5} s^{-1}) at 0 h (top left), 72 h in EXP(1, 0) (top right), 72 h in EXP(0, 1) (bottom left) and 72 h in EXP(1, 1) (bottom right). Areas with negative value are shaded.

tropical storm genesis (Kurihara and Tuleya, 1981; Figs. 6 and 8).

b. Structure of disturbances at 72 h

In this subsection, various fields after 72 h integration in EXP(1, 0), EXP(0, 1) and EXP(1, 1) are presented on an x–p cross section together with their initial patterns (Figs. 3–6). Each figure is prepared so that the position of the surface vorticity maximum coincides with the midpoint of the bottom side of a cross section.

Figure 3 shows distributions of the relative vorticity. It is indicated that the shape of the disturbance is well preserved in EXP(1, 0) while its amplitude decreases. In EXP(0, 1), the extent of positive vorticity region at each pressure level is maintained because the dynamics governing the system are linear. However, the vertical tilt of the wave axis is modified by the heating effect. As a result, the eastward phase shift of vorticity maximum at 300 mb relative to the surface trough decreases from 193° at the initial time to 108° at 72 h.

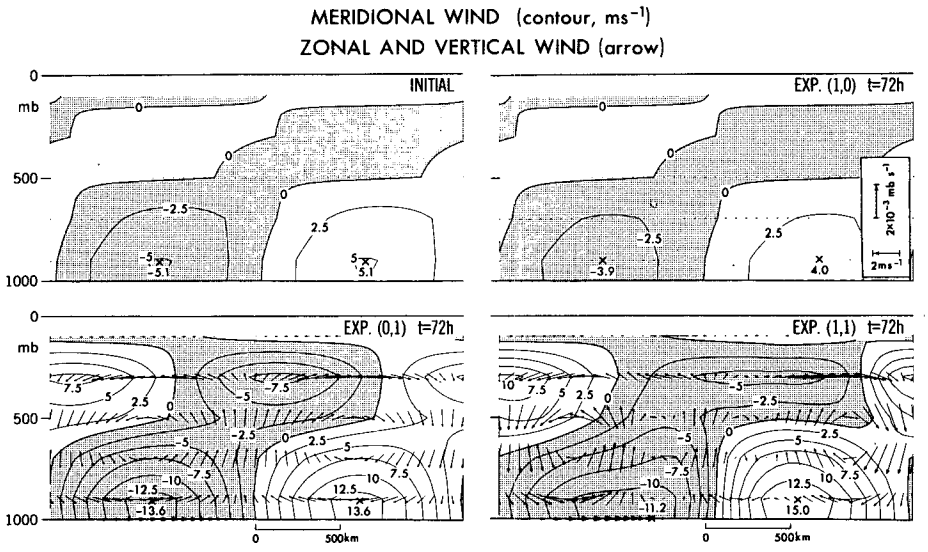

FIG. 4. As in Fig. 3, but for the meridional wind component (contour, m s^{-1}) and zonal-vertical wind component (arrow). Zonal wind shown is the perturbation component only. Arrows are obtained from proper projection of the wind components u and ω onto 2500 km × 1000 mb frame domain.

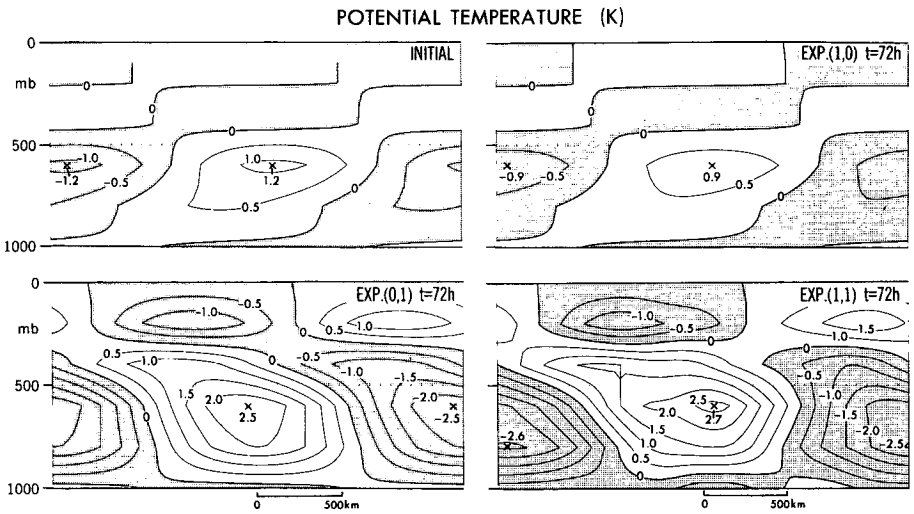

FIG. 5. As in Fig. 3, but for the perturbation potential temperature (K).

In the case of EXP(1, 1) the aforementioned phase shift at 72 h is 144° and, in contrast to EXP(0, 1), a concentration of the positive vorticity area occurs. At the surface, the zonal extent of the area with cyclonic vorticity is reduced from 1250 km, i.e., the half wavelength at 0 h to 875 km. At the same time, the cyclonic vorticity is intensified while the anticyclonic vorticity is decreased compared with those in EXP(0, 1). A nonlinear term $-(u\zeta)_x$ in (1) can be split into the nonlinear zonal advection term $-u\zeta_x$ and the nonlinear vorticity stretching term $-\zeta D$. If the ζ and D-fields are 180° out of phase from each other, the wind u is directed from the position of minimum vorticity to that of maximum vorticity. Accordingly, the advection of ζ by the wind u causes the shrinking of the area with positive ζ and the broadening of the area with negative ζ. It is obvious that the vorticity stretching term in this case yields a positive tendency everywhere, meaning the increase of maximum (positive) ζ and the reduction of the magnitude of minimum (negative) ζ. Thus, the combined effects of advection and stretching can make a positive vorticity part smaller and more intense and a negative one larger and weaker. As mentioned before, these tendencies caused by nonlinearity become effective only when the mass field changes in such a way as to preserve a state of nearly geostrophic balance.

The perturbation flow fields at 72 h in the three experiments are presented in Fig. 4. The distribution of the meridional component, which defines the vorticity field, reveals some interesting features. For example, the vertical tilt of a wave trough, i.e., the

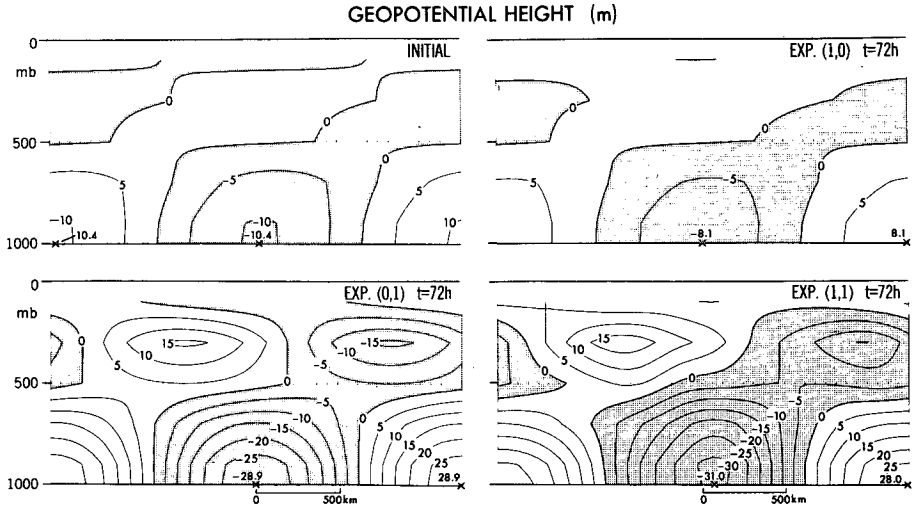

FIG. 6. As in Fig. 3, but for the perturbation geopotential height (ϕ/g; in m).

slope of the zero contour for v, is eastward with increasing height in the lower layer of a free wave and also in EXP(1, 0). Such a tilt is nearly vertical at 72 h in the two experiments that include the heating effect. Also, the region of northerly flow at upper levels shifts to the west in these experiments. It should be noted that the large increase of positive vorticity at 1000 mb in EXP(1, 1) as compared with EXP(0, 1) is a result of the contraction rather than the magnitude increase of the v-field; specifically, the 27.2 m s^{-1} difference between the maximum v and the minimum v in EXP(0, 1) takes place over the 1250 km distance, while the 26.2 m s^{-1} difference is observed in EXP(1, 1) over the 875 km span. The above feature of the v-field is similar to that shown by Hoskins (1975, Fig. 1) in regard to the frontogenesis. An obvious effect of the heating is to intensify the zonal–vertical circulation as shown by arrows in Fig. 4. In EXP(0, 1), the low-level convergence and divergence are associated with the surface trough and ridge, respectively. This is also the basic feature of the circulation in EXP(1, 1) although it is partially masked in Fig. 4 by secondary features.

In the developed disturbances in EXP(0, 1) and EXP(1, 1), an intensified surface vorticity maximum is located at or near the position of surface pressure minimum. This implies the existence of warm air above the area with large surface vorticity. Figure 5 and 6, in which the zonal–vertical distributions of the perturbation potential temperature and the geopotential height are respectively presented, clearly show that the air above the deepened surface low is warm. The warming in these experiments is almost entirely associated with the diabatic heating. The temperature change due to the meridional advection [the term Bv in (6)], is small in the present model. The surface pressure minimum in EXP(1, 1), estimated from the geopotential height, decreases by 2.4 mb in 72 h, which is only slightly larger than the 2.2 mb deepening in EXP(0, 1). We again notice a westward shift of the upper-level trough relative to the surface low in the case of the developed disturbances.

c. *Some features of a developing disturbance*

In EXP(1, 1), a linear free wave at the initial time evolves into a thermally-forced, developing disturbance which consists of many components with different space and time scales. It is of interest to examine how long a developed system can be sustained without the nonlinearity effect or the diabatic heating. In order to investigate the above problem, integrations were carried out in which either or both nonlinearity and heating processes were removed from EXP(1, 1) at 36 h.

Figure 7 shows the time variations of the maximum relative vorticity at 1000 mb in the above additional

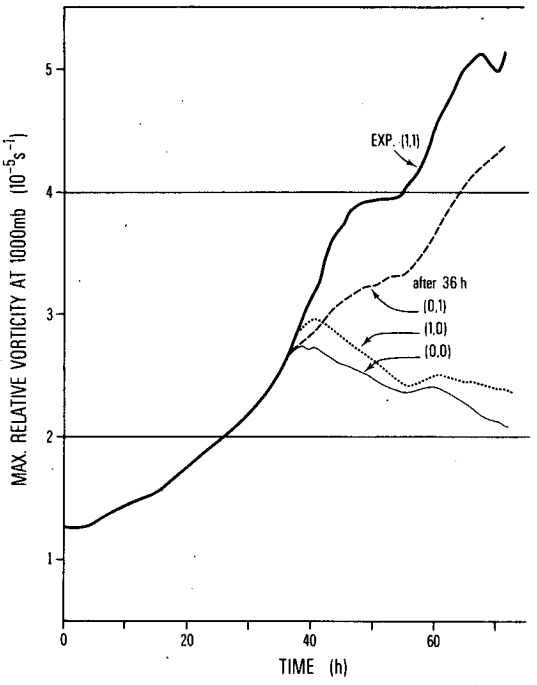

FIG. 7. Time variations of the maximum relative vorticity at 1000 mb for EXP(1, 1) (thick solid line); the integration without the nonlinear effect after 36 h [dashed line: (0, 1)]; the integration without heating after 36 h [dotted line: (1, 0)]; and the integration with neither nonlinear effect nor heating after 36 h [thin solid line: (0, 0)].

experiments. It is shown that the development ensues with the effect of heating alone (a dashed line in the figure). However, the development rate in this case is less than that in EXP(1, 1). With the nonlinearity effect alone, the disturbance continues to grow until 41 h, when it starts to decay (a dotted line in Fig. 7). This course of events indicates that the nonlinearity process can contribute to wave growth, but it becomes ineffective without the support of the heating effect. When the effects of both nonlinearity and heating are removed, the disturbance immediately tends to weaken (a thin solid line in Fig. 7). Further analyses reveal that the disturbance in this case undergoes a noticeable structural change throughout the period of decay. For example, the phase difference between the upper and lower-level vorticity fields is reduced from 180° at 36 h to 72° at 72 h.

4. Experiments with different basic flows and waves

In this section, it will be shown that the qualitative features of wave transformation described in the preceding section are shared among three different disturbances under various basic flow conditions. We prepared 15 different cases through the combination of five basic flows having different vertical shear and three waves with different structures. For each of the 15 cases, three time integrations equivalent to EXP(1,

0), EXP(0, 1) and EXP(1, 1) as defined in Table 2 were performed.

In Table 3, the profiles of the five basic flows used in these supplemental experiments are shown: the winds with easterly shear E1 and E2, with westerly shear W1 and W2, and without vertical shear Z. The magnitude of shears for E2 or W2 is greater than that for E1 or W1, respectively. We note here that some preliminary experiments indicated that the addition of a vertically uniform mean flow to the above profiles has very little impact on the behavior of the waves in the present model. However, the impact of a mean basic flow in a more comprehensive three-dimensional model can be significant (Tuleya and Kurihara, 1981; Section 7b). The initial disturbance for the model is one of the three waves, hereafter referred to as Waves A, B and C; each wave represents a normal mode of three different types of systems. The basic flows used to determine the waves, the phase speeds and the *e*-folding times of the waves are listed in Table 4. Note that the basic flows which carry the waves in the supplemental integrations are independently specified in Table 3. Wave A is identical to the wave used in the primary experiment in Section 3. Wave B is a normal mode of the system with a uniform easterly without vertical shear, while Wave C is that of the system with the surface easterly and westerly flow aloft. All three waves have the same wavelength of 2500 km. They are specified to give the same vorticity maximum of 1.25×10^{-5} s^{-1} at the initial time at the 1000 mb level. The amplitude of the vorticity is fairly small above the 500 mb level in Wave A and above the 300 mb level in Wave C. For Wave B, the vorticity field with the amplitude of 1.08×10^{-5} s^{-1} and with an opposite sign to the low-level fields exists above the 300 mb level. The pressure fields of all three waves are negatively correlated to the vorticity fields at all levels. The wave trough tilts to the east with height, ~95 km between the 1000 and 700 mb levels in Wave A, ~135 km in Wave B and ~90 km in Wave C. The surface convergence is generally associated with the positive vorticity. The locations of the surface convergence maxima are 55 km west, 50 km east, and 200 km east of those of the surface vorticity maxima in Waves A, B and C; this means that the diabatic heating, when incorporated into the model, is largest to the west of the 700 mb trough in Waves A and B and to the east in Wave C. Among the three waves, Wave B seems to be most similar to the easterly waves described by Reed (1979).

Three experiments, i.e., EXP(1, 0), EXP(0, 1) and EXP(1, 1) were performed with respect to each of the aforementioned three waves for five different basic flow conditions. Results of these integrations are presented in Table 5. The obtained results clearly show that the argument made in the preceding section also holds in general under the different mean flow conditions and wave structures. Namely, the easterly wave hardly intensifies with the addition of only the nonlinear effect acting on a vertical plane: the maximum vorticity decreased in EXP(1, 0) in 13 out of 15 cases and increased in two cases but only by two and five percent of the initial value. The diabatic heating is a necessary ingredient for the increase of

TABLE 3. Vertical profiles of five different basic flows. Shear given in m s^{-1}.

Height (mb)	Easterly shear E2	Easterly shear E1	No shear Z	Westerly shear W1	Westerly shear W2
100	−12	−7	0	7	12
300	−10	−6	0	6	10
500	−6	−4	0	4	6
700	−2	−2	0	2	2
900	0	0	0	0	0
1000	0	0	0	0	0

TABLE 4. The basic flows used to determine the waves. Phase speeds and the *e*-folding times of the waves are also listed.

Wave	Basic flow (m s^{-1}) (mb) 100	300	500	700	900	1000	Phase speed (m s^{-1})	*e*-folding time (h)
A	−12	−11	−9	−7	−5	−5	−8.9	−288.4
B	−5	−5	−5	−5	−5	−5	−8.0	−363.1
C	2	1	−1	−3	−5	−5	−6.6	−170.1

TABLE 5. Maximum relative vorticities at the 1000 mb level at 36 h: for Waves A, B and C, three integrations each, i.e., EXP(1,0), EXP(0,1) and EXP(1,1), were carried out under five different vertical shears of basic flow. The difference between the basic flow at 500 mb (U_{500}) and the phase velocity of the surface vorticity at 1000 mb (c) in EXP(0,1) is also listed for each combination of wave types and basic flow conditions.

Experiment	Vertical profile of basic flow E2	E1	Z	W1	W2
Wave A					
EXP(1,0) (10^{-5} s^{-1})	1.16	1.14	1.04	0.98	0.97
EXP(0,1)	2.12	2.08	1.82	1.71	1.73
EXP(1,1)	3.11	2.87	1.76	2.39	2.67
$U_{500}-c$ (m s^{-1})	−1.4	0.6	2.2	3.8	5.3
Wave B					
EXP(1,0) (10^{-5} s^{-1})	1.27	1.31	1.16	1.01	0.95
EXP(0,1)	2.47	2.49	2.06	1.77	1.70
EXP(1,1)	4.89	4.28	2.11	2.69	2.88
$U_{500}-c$ (m s^{-1})	−0.5	−1.1	2.4	3.8	5.3
Wave C					
EXP(1,0) (10^{-5} s^{-1})	1.16	1.20	1.09	1.01	0.98
EXP(0,1)	2.11	2.14	1.86	1.72	1.70
EXP(1,1)	4.12	3.62	1.91	2.13	2.52
$U_{500}-c$ (m s^{-1})	−0.9	0.6	2.2	3.5	5.3

vorticity maxima at the surface; results from EXP(0, 1) and EXP(1, 1) in all 15 cases support this contention. The nonlinearity process can make positive contribution to the wave transformation in the presence of heating: the value for EXP(1, 1) in Table 5 is greater than that for EXP(0, 1) in 14 out of 15 cases. Such a contribution of the nonlinearity is, however, not large in the cases of the basic flow of the profile Z. During the integrations in these cases, the convergence field tended to be 90° out of phase relative to the vorticity field, making the nonlinear effect rather minimal.

It is interesting to see in Table 5 that, in the case of EXP(0, 1), all of Waves A, B and C intensify more in the basic flow with easterly vertical shear than in the one with westerly shear. Tuleya and Kurihara (1981) note that the coupling of the upper-level basic flow and the propagating low-level disturbance is an important factor in keeping the warm area above the disturbance and thereby maintaining a favorable condition for the growth of the disturbance. The difference between the basic wind at 500 mb and the phase velocity c of the vorticity field at 1000 mb, listed in Table 5, is a measure of such a coupling. Indeed, the surface vorticity increase in EXP(0, 1) is relatively large under the wind profiles E1 and E2 for which the vertical coupling is strong. The existence of the preferred shear is apparently related to the fact that easterly waves intrinsically move westward. Such a dependency of the wave transformation on the basic wind profile is carried over to EXP(1, 1), although it becomes a little obscure: the maximum vorticity of each wave in EXP(1, 1) under the easterly shear condition is relatively large as compared with that under the westerly shear condition.

The above results are in qualitative agreement with those obtained from the three-dimensional model (Tuleya and Kurihara, 1981). A point to be made is that the sensitivity of wave evolution on the state of basic flow is considerably enhanced in a three-dimensional simulation; for instance, formation of a tropical depression did not occur in the three-dimensional model in the case of strong westerly shear even though the heating effect was present.

5. Summary and remarks

In this study, the roles of the nonlinear process on the vertical plane and of the diabatic heating in the transformation of a tropical easterly wave were investigated through time integrations of a simple numerical model. It was found that a model free wave resembling an easterly wave can be made intense by a CISK-type heating: EXP(0, 1). The nonlinear dynamics alone, which include nonlinear zonal advection and vertical stretching of relative vorticity, have little impact on the wave evolution: EXP(1, 0). However, the nonlinearity effect can enhance the wave development if it is properly combined with sufficient diabatic heating: EXP(1, 1). In this case, the fields of surface vorticity and divergence are coupled so that the interaction leads to the contraction and deepening of the surface trough of an easterly wave, possibly leading to the formation of a distinct vortex, i.e., a tropical depression. Sustained increase of vorticity at the surface seems to require concurrent warming of the air above the surface vorticity maximum, for this tends to maintain the perturbation flow in the geostrophic balance and channels the released energy into the Rossby wave mode. Since this mode propagates intrinsically to the west, it is favorable for wave growth that the basic flow have an easterly shear, which will advect warmed upper air in the same sense as the phase propagation of the wave.

Within the developed disturbances in the present experiments, forced deformation of the initial wave structure was found. It should be noted here that the heat is externally given in EXP(0, 1) and EXP(1, 1). Such a forced system may be contrasted to a system in which the heating effect is a built-in property of the normal modes. In the latter system, a free wave, analogous to an easterly wave of the primary experiment, is found to be an amplifying wave with an e-folding time of 188.5 h. Starting at the same initial value as in the present study, the maximum surface vorticity of this wave increases to 1.88×10^{-5} s^{-1} at 72 h, which is only about 56% of the vorticity of the forced wave in EXP(0, 1). The vorticity field in this free wave shows 83° phase angle difference between the 300 and 1000 mb levels, as compared with 193° in the adiabatic normal mode, EXP(0, 0). Structural differences among the adiabatic free wave, a free wave including the heating effect and a wave modified by external forcing are an interesting topic in the study of the evolution of disturbances as well as in the problem of normal mode initialization of meteorological fields. (Note that each of the first two waves mentioned previously represents a single normal mode, while the third wave consists of more than one normal mode.)

The heating in the present model takes a wave CISK-type form with the effect of surface friction included. A problem related to a CISK-type formulation of the heating effect is that the growth rate of a wave increases as the scale of the wave decreases unless mechanisms to suppress short waves exist. This difficulty is a great concern to some numerical modelers. When the integration for EXP(1, 1) of the primary experiment was extended, small-scale fluctuations started to appear in the vorticity field after about 90 h, perhaps partly because the short waves in the present model can take up the latent energy indefinitely. In addition, the condition of slab symmetry used in this study does not allow the formation of a flow field with finite meridional scale. Consequently, the time integration of the present model beyond a certain stage of wave evolution becomes

physically less meaningful. Nevertheless, we believe that the results of the previously discussed integration before 72 h exhibit main features of the transformation of easterly waves reasonably well. One conclusion of the present study is that the heating effect is a necessary ingredient for the genesis of tropical depressions. This is in good agreement with the numerical simulation study by Kurihara and Tuleya (1981) as well as with the observational analysis of waves in the western Pacific (e.g., Wallace, 1971).

The nonlinearity effect discussed in this paper may well account for the midlatitudes frontogenesis in a baroclinic wave (e.g., Hoskins, 1975). The present study suggests that, in the course of the development of a mesoscale system, the warming above the surface perturbation has to be concurrent with the surface vorticity increase. Noting the typically observed tilt of a cold front with height, we conjecture that the warm air advection from the south contributes to the required warming in this case. This effect is expressed by the term Bv in (6) and can be of significance at midlatitudes. A front may form even without the adiabatic heating effect. This is in sharp contrast to the tropical cyclogenesis for which the release of latent heat seems to be essential.

Acknowledgments. The authors are grateful to G. P. Williams and R. E. Tuleya, GFDL/NOAA, and K. Puri, GFD Program, Princeton University, for valuable comments on the earlier version of the manuscript. They thank H. E. Willoughby, HRD/AOML/NOAA, and the reviewers of this paper for constructive criticism and many helpful comments. Thanks are also due to J. Kennedy, J. Conner, and P. Tunison for their assistance in the preparation of the manuscript. The work of the second author was supported by the National Science Foundation under Grant ATM-7719955.

REFERENCES

Hoskins, B. J., 1975: The geostrophic momentum approximation and the semigeostrophic equations. *J. Atmos. Sci.*, **32**, 233–242.

Kurihara, Y., 1976: On the development of spiral bands in a tropical cyclone. *J. Atmos. Sci.*, **33**, 940–958.

——, and G. J. Tripoli, 1976: An iterative time integration scheme designed to preserve a low-frequency wave. *Mon. Wea. Rev.*, **104**, 761–764.

——, and R. E. Tuleya, 1981: A numerical simulation study on the genesis of a tropical storm. *Mon. Wea. Rev.*, **109**, 1629–1653.

Reed, R. J., 1979: The structure and behaviour of easterly waves over West Africa and the Atlantic. *Meteorology over the Tropical Oceans*, D. B. Shaw, Ed., Roy. Meteor. Soc., 57–71.

Shapiro, L. J., 1977: Tropical storm formation from easterly waves: A criterion for development. *J. Atmos. Sci.*, **34**, 1007–1021.

Tuleya, R. E., and Y. Kurihara, 1981: A numerical study on the effects of environmental flow on tropical storm genesis. *Mon. Wea. Rev.*, **109**, 2487–2506.

Wallace, J. M., 1971: Spectral studies of tropospheric wave disturbances in the tropical western Pacific. *Rev. Geophys.*, **9**, 557–612.

Yanai, M., 1961: A detailed analysis of typhoon formation. *J. Meteor. Soc. Japan*, **39**, 187–214.